



CHORUS

This is the accepted manuscript made available via CHORUS. The article has been published as:

Asymmetric switchinglike behavior in the magnetoresistance at low fields in bulk metamagnetic Heusler alloys

Tapas Samanta, Ahmad Us Saleheen, Daniel L. Lepkowski, Alok Shankar, Igor Dubenko, Abdiel Quetz, Mahmud Khan, Naushad Ali, and Shane Stadler

Phys. Rev. B **90**, 064412 — Published 11 August 2014

DOI: [10.1103/PhysRevB.90.064412](https://doi.org/10.1103/PhysRevB.90.064412)

**Asymmetric switching-like behavior in the magnetoresistance at low-fields in bulk
metamagnetic Heusler alloys**

Tapas Samanta¹, Ahmad Us Saleheen¹, Daniel L. Lepkowski¹, Alok Shankar¹, Igor
Dubenko², Abdiel Quetz², Mahmud Khan³, Naushad Ali², and Shane Stadler¹

¹Department of Physics & Astronomy, Louisiana State University, Baton Rouge, LA 70803
USA

²Southern Illinois University, Carbondale, IL 62901 USA

³Department of Physics, Miami University, Oxford, OH 45056 USA

A novel physical phenomenon has been observed that resembles a large asymmetric switching-like magnetoresistance at low applied fields in *bulk* metamagnetic Heusler alloys. A thermally-activated isothermal forward metamagnetic transition with a signature of a pronounced time-dependent relaxation was observed in a *bulk* B-substituted off-stoichiometric Ni-Mn-In Heusler alloy, whereas the reverse metamagnetic transition exhibited the usual athermal behavior with no thermal activation. The asymmetry between the forward and reverse metamagnetic transitions resulted in a large switching-like, low-field magnetoresistance ($\sim 16\%$ for a field change of $B=0 \rightarrow 0.25$ T at $T=304$ K) in the *bulk* Heusler alloys, $\text{Ni}_{50}\text{Mn}_{35}\text{In}_{15-x}\text{B}_x$ ($1 \leq x \leq 2$).

Keywords: asymmetric magnetoresistance, bulk metamagnetic Heusler alloys

PACS number(s): 72.15.Gd, 75.30.Kz, 76.60.Es, 75.30.Sg

I. INTRODUCTION

An asymmetric resistance switching in small magnetic fields, i.e., a large low-field magnetoresistance (MR), usually attributed to the difference of spin-dependent scattering of conduction electrons associated with the relative changes of the orientation of the adjacent magnetic layers with respect to the direction of applied magnetic field, has been observed in artificial magnetic multilayer heterostructures, such as spin-valves and magnetic tunnel junction. [1-7]. Magnetic multilayer structures based on Heusler alloys have been shown to exhibit a similar type of MR behavior [5]. However, to realize a large, low-field asymmetric MR in *bulk* materials is quite unusual. The symmetric character of direct and reverse metamagnetic transitions, both usually athermal in nature, possibly preclude the observation of asymmetric magnetoresistance behavior in *bulk* systems. Moreover, phenomena associated with the kinetic arrest of a metastable phase (e.g., the ferromagnetic austenitic phase in the case of the material reported here) in the vicinity of or below a magnetostructural transition (MST) may also hinder the abovementioned switching behavior in the case of bulk systems. A different mechanism was responsible for the spin-valve-like MR observed in *bulk* Mn_2NiGa Heusler alloys; this was explained as a result of antisite coupling of Mn atoms located in the Ga positions, forming ferromagnetic nanoclusters coupled antiferromagnetically to the other Mn atoms [8].

Changes in the magnetic and structural phase balance affect the character and dynamics of the MST, and can result in a non-ergodic, magnetic-glass-like dynamical response [9]. Most often such field-induced heterogeneity is relatively stable with respect to time in certain temperature and magnetic field intervals [9]. In the present study, we report a large asymmetric, switching-like low-field MR, a behavior similar to that observed in magnetic multilayers, in *bulk* $\text{Ni}_{50}\text{Mn}_{35}\text{In}_{15-x}\text{B}_x$. In this case, the large asymmetric MR is associated with a thermal-fluctuation-assisted de-arrest of a fraction of the metastable phase

due to the isothermal nature of the forward metamagnetic transition from a ferromagnetic (FM) austenite to a paramagnetic-like (PM) martensitic phase (indicating a disordered magnetic state in martensitic phase), whereas the reverse transition is as usually observed, athermal. A model is proposed based on a phenomenological Landau-type free energy diagram in order to elucidate the unusual asymmetric MR behavior in *bulk* $\text{Ni}_{50}\text{Mn}_{35}\text{In}_{15-x}\text{B}_x$ Heusler alloys.

II. EXPERIMENTAL DETAILS

Polycrystalline $\text{Ni}_{50}\text{Mn}_{35}\text{In}_{15-x}\text{B}_x$ ($x=1.0, 1.5, \text{ and } 2.0$) samples were prepared by arc-melting the constituent elements Ni, Mn, In, and B of purities 99.995, 99.9998, 99.9999, and 99.5%, respectively, in an ultra-high purity argon atmosphere. The samples were annealed in high vacuum ($\approx 10^{-5}$ torr) for 24 hours at 850°C . The crystal structures of the samples were determined using a room temperature X-ray diffractometer (XRD) employing Cu $K\alpha$ radiation. A superconducting quantum interference device magnetometer (SQUID, Quantum Design MPMS) was used to measure the magnetization of the samples in a temperature interval of 10-380 K, and in applied magnetic fields (B) up to 5 T. All samples were cooled from 380 to 10 K at zero magnetic field (ZFC) prior to the magnetization measurements. Magnetic measurements under hydrostatic pressure were performed in a commercial BeCu cylindrical pressure cell (Quantum Design). Daphne 7373 oil was used as the pressure transmitting medium. The value of the applied pressure was calibrated by measuring the shift of the superconducting transition temperature of Pb used as a reference manometer ($T_C \sim 7.2$ K at ambient pressure) [10]. The temperature dependence of the resistivity (ρ) in zero-field as well as in a 5 T magnetic field was measured using the conventional four-probe method. The isothermal magnetoresistance [$\text{MR} = \{(\rho(H) - \rho(0)) / \rho(0)\} \times 100$] measurements at different constant temperatures were carried out in magnetic fields up to ± 5 T.

III. EXPERIMENTAL RESULTS

The room temperature X-ray diffraction (XRD) patterns of $\text{Ni}_{50}\text{Mn}_{35}\text{In}_{15-x}\text{B}_x$ are shown in Fig. 1. The system is predominantly in the low-temperature martensitic phase with traces of the high-temperature austenitic phase, which has been detected for all of the studied B-concentrations ($x=1.0, 1.5, \text{ and } 2.0$). The observed XRD pattern is typical for Ni-Mn-In based Heusler alloys in the phase coexistence region exhibiting a MST near room temperature.

The temperature-dependent resistivity (ρ) data at zero-field, and in the presence of a 5 T magnetic field employing a zero-field-cooled (ZFC) protocol, are shown in Fig. 2. In the vicinity of the MST (occurring at $T=T_M$) from a PM-like martensitic (PMM) phase to a FM austenitic (FA) phase, as evident from the ZFC $M(T)$ curves measured at $B=0.05$ T (Fig. 2), the increase of ρ was found to be $\sim 280, 220, \text{ and } 196 \mu\Omega \text{ cm}$ for $x=1.0, 1.5, \text{ and } 2.0$, respectively, in the PMM phase, which is about two times larger than that observed in the FA phase (where $\rho \sim 150, 122, \text{ and } 111 \mu\Omega \text{ cm}$ for $x=1.0, 1.5, \text{ and } 2.0$, respectively). An applied magnetic field of 5 T resulted in a decrease of T_M by about 7 K for all concentrations.

It is interesting to point out that T_M shifts to higher temperature with increasing B concentration. The isoelectronic substitution of the smaller B atoms for In in $\text{Ni}_{50}\text{Mn}_{35}\text{In}_{15-x}\text{B}_x$ possibly acts as an effectively positive chemical pressure (P), resulting in a shift of T_M to higher temperature with increasing B substitution. A similar type of increase in T_M was reported for other B-substituted Heusler alloys, such as $\text{Ni}_2\text{Mn}(\text{GaB})$ [11] and $\text{Ni}_{50}\text{Mn}_{36.5}\text{Sb}_{13.5-x}\text{B}_x$ [12]. For further verification, $M(T)$ data at $B=0.05$ T for $x=1$ were collected under the application of hydrostatic pressure (shown in Fig. 3). A shift of T_M by about 11 K to higher temperature was detected for $P=7.7$ kbar with respect to ambient pressure. Therefore, the chemical pressure induced by B substitution and the physical hydrostatic pressure play similar roles in displacing T_M to higher temperature. In contrast to

the effects of pressure, an applied magnetic field decreases T_M as shown in Fig. 3 (right axis), resulting in a decrease of T_M by about 7 K for a field change of 5 T.

The thermal variation of the MR is shown in Fig. 4(a), which was calculated from the temperature-dependent resistivity data measured at $B=5$ T and at zero-field. Large MR values of 54, 50, and 46% were observed for a field change of $\Delta B=5$ T in the vicinity of the MST for $x=1.0$, 1.5, and 2.0, respectively. Importantly, the evaluated maximum values of the MR, as determined from the field-dependent isothermal resistivity measurements (plotted in Fig. 4(b-c) and 5(a-d)), are in good agreement with the values of the MR calculated from $\rho(T)$ data in the presence of a constant magnetic field.

Selected isothermal $MR(B)$ and $M(B)$ curves in close vicinity to the MST for $x=1$ are depicted in Fig. 5. The sample was first zero-field-cooled from 360 to 250 K to ensure a complete martensitic state, and then zero-field-heated to the test temperatures on the border of the MST temperature range. With increasing magnetic field (Fig. 5, path 1: $0 \rightarrow B_{\max}$) both $MR(B)$ and $M(B)$ exhibit a magnetic-field-induced reverse metamagnetic transition from a PMM to a FA phase. However, the virgin $MR(B)$ and $M(B)$ curves both lie outside the subsequent field cycling path. As the temperature moves into the phase coexistence region in the vicinity of the MST, the difference between zero-field ρ before and after first field cycling increases, which is related to the kinetic arrest of the fractional metastable FA phase as reported for other Ni-Mn-X based Heusler alloys [13, 14]. The $M(B)$ curve also shows evidence of the arrested FA phase as the increasing value of the low-field magnetization after field cycling relative to the virgin curve (see paths 1 and 5 in Fig. 5(e-f)). Therefore, it is expected that the field-induced arrested FA phase should result in a decrease of ρ and MR; the decreases of MR with the reduction of B (from $B=5$ T to 0) are 4, 8, 35, and 33% for $x=1$ at $T=300$, 302, 304, and 305 K, respectively (shown in Fig. 5(a-d)), are due to a reduced scattering probability of conduction electrons in the FM phase. Interestingly, instead of a

further decrease, a sharp *increase* in the MR results in an asymmetric switching-like MR behavior with the application of a low reversal field for $x=1$ ($\sim 16.5\%$ for $\Delta B=0.25$ T at 304 K). This type of asymmetric MR behavior, usually attributed to the spin-dependent scattering of conduction electrons, has been observed in artificial magnetic multilayer heterostructures, such as spin-valves and magnetic tunnel junction. [1-7]. It is especially interesting to observe this type of behavior in a *bulk* system.

To shed more light on the observed unusual asymmetric MR behavior, a time-dependent magnetization relaxation study was performed in the vicinity of both field-induced reverse and forward metamagnetic transitions close to the MST, the data of which are shown in Fig. 6 for $x=1$ and $T=304$ K. The $M(t)$ curves for reverse and forward metamagnetic transitions show stark differences. A slower relaxation behavior has been detected in the vicinity of the reverse metamagnetic transition, which is typical for this class of materials in the vicinity of the phase coexistence region (i.e., a low-temperature PMM phase and a metastable high-temperature FA phase in this system) due to the formation of a magnetic-glass state associated with the kinetic arrest of the metastable FA phase [9, 13, 14]. In contrast to the reverse transformation, a rapid pronounced relaxation has been observed in the vicinity of forward metamagnetic transition, which corresponds the isothermal nature of the forward metamagnetic transition [15]. The normalized $M(t)$ curve in the vicinity of isothermal forward metamagnetic transition can be well-fitted by a logarithmic dependence (suggesting a broad distribution of activation energies as well as energy barriers) as $M(t)/M(t=0)=1-Z\ln[(t+t_0)/t_0]$, where Z is the magnetic viscosity coefficient and t_0 is a positive constant used to avoid the logarithmic divergence at $t=0$. On the basis of thermal fluctuation aftereffects, Z can be expressed as $Z \propto N \langle M \rangle k_B T$, where N is the amount of transforming material and $\langle M \rangle$ is the change of average magnetization per unit amount of phase transformation. Therefore, a larger value of Z for the isothermal forward metamagnetic

transition (see inset of Fig. 6) indicates a larger fraction of the sample transforming from the FA to the PMM phase due to thermal-fluctuation-assisted destabilization of the FA phase, and concurrent nucleation of the PMM matrix at the expense of the FA phase. Thus, the relaxation study of this system indicates that the forward metamagnetic transition from FA to PMM is isothermal with pronounced magnetic relaxation, whereas the reverse transition (from PMM to FA) is the usual athermal transformation with a slow, glassy-like relaxation.

IV. DISCUSSION

A. Origin of asymmetric magnetoresistance

As evident from the magnetic relaxation behavior, the field-dependent evolution of the free-energy profiles must be completely different in nature for reverse and forward metamagnetic transitions, as represented in Fig.7(a) and (b), respectively. For athermal reverse metamagnetic transitions, as commonly reported to describe this class of studied Heusler alloys, the free energy minimum corresponding to the FM austenitic phase decreases with increasing B due to the change in magnetic energy by amount $-\delta(BM)$. Progressively more of the PM-like martensitic phase transforms to the FM austenitic phase with increasing B . An athermal forward metamagnetic transition, as most commonly observed with decreasing B in these system, can only result in a symmetric type of inverse metamagnetic transition by transforming the FM austenitic phase to the PM-like martensitic phase (for instance, by ignoring the kinetic arrested phenomena), leading to a symmetric MR behavior. However, if the forward metamagnetic transition occurs in close vicinity to $B=0$, and a reversal of B can recover the initial low-magnetization martensitic state (as observed in our studied system; see the low-field magnetization of path 3 and 5 in Fig. 5(e-f)), the athermal character of the phase transition cannot explain an asymmetric switching-like change in MR.

Usually, the FM austenitic phase undergoes a kinetic arrest after a field-induced, reverse metamagnetic transition and presents as a non-ergodic, magnetic-glass-like dynamical

response which is relatively stable with respect to time in certain temperature and magnetic field intervals [9]. Moreover, the application of a reverse field again starts to stabilize the FM austenitic phase associated with the minimization of free energy. Therefore, in the case of an athermal forward metamagnetic transition, the transformation from the FM austenitic to the PM-like martensitic phase is a forbidden response to the application of a reverse field, provided there is no unidirectional anisotropy associated with the system that can result in exchange bias for the phase-coexisted system, similar to that observed in our studied materials. In $\text{Ni}_{50}\text{Mn}_{35}\text{In}_{15-x}\text{B}_x$, no signature of exchange bias has been observed in the vicinity of the MST.

As evident from the present relaxation study, for the thermally-activated isothermal behavior (as opposed to the more common athermal character) of the forward metamagnetic transition with a signature of pronounced time-dependent relaxation, the free-energy barrier between the austenite and martensite phases can be overcome isothermally with the assistance of thermal fluctuations (for simplicity, the model is described considering a single energy barrier, instead of a logarithmic dependence of relaxation which is associated with a broad distribution of energy barriers and activation energies). In this case, thermal fluctuations destabilize the FM austenitic phase, resulting in the nucleation of the PM-like matrix at the expense of the FM austenitic phase. Therefore, a transformation from the FM austenitic to the PM-like martensitic phase is possible for an isothermal forward metamagnetic transition, as depicted in Fig. 7(b), which leads to an asymmetric, switching-like change of MR associated with the stabilization of the PMM martensitic phase with the application of a small reversal field. It has been found that a small amount of the FM austenitic phase fraction kinetically arrested after the reverse metamagnetic transition, which is not recoverable isothermally. However, the most stunning observation is that the

isothermal nature of the forward metamagnetic transition results in a large switching-like, low-field MR (~16%) for a field change of $B=0 \rightarrow 0.25$ T near room temperature (304 K).

In the case of a spin-valve, the difference between the spin-dependent scattering of conduction electrons in the two different magnetization geometries (low ρ for ferromagnetic alignment of layers due to a small scattering probability, and high ρ for antiferromagnetic layer alignment associated with an enhanced scattering probability) results in a switching-like change in the MR. The presently studied system with $x=1$ shows a higher value of ρ in the presence of small magnetic field ($B=0.25$ T and $T=304$ K) due to the growth of a low-temperature PMM phase associated with the thermal-fluctuation-assisted de-arrest of a fractional metastable FA phase. However, the presence of a relatively large fraction of the metastable FA phase at zero-field that arises from field cycling results in a low value of ρ at zero-field. The net result is that a large asymmetric switching-like MR (~16%) has been observed even in *bulk* polycrystalline $\text{Ni}_{50}\text{Mn}_{35}\text{In}_{15-x}\text{B}_x$ with $x=1$, due to the de-arrest of the metastable FA phase and a concurrent nucleation of the PMM phase. It should be noted that we cannot exclude the possibility of other sources of scattering, namely electron-lattice scattering, which can contribute to the MR of a system that has coexisting phases with different crystallographic structures.

B. Effect of electron-spin and electron-lattice scattering on magnetoresistance

In the following, a rough estimation has been made of the relative contributions originating from two different types of scattering processes, i.e., electron-spin and electron-lattice. This has been done in terms of the relative contributions from the magnetic entropy change (ΔS_M), as related to changes in magnetic configuration, and the structural entropy change (ΔS_{st}) to the total entropy change (ΔS_{tot}) associated with the MST. It would be expected that the MR is affected by the changes of magnetic configuration or crystallographic structure, similar to their influences on the entropy change. A proportional relationship

between MR and ΔS_{tot} has been reported for other metallic ferromagnets in the vicinity of their ferromagnetic Curie temperatures [16]. For materials exhibiting a MST, the relationship between MR and ΔS_{tot} is not straightforward, however the relative weighting of the changes of the two different physical quantities, i.e., the magnetic orientation and structure, is expected to similarly effect both the MR and ΔS_{tot} . In fact, a linear relationship between MR and ΔS_{tot} has been observed at low fields in our system with $x=1$.

For a MST, the ΔS_{tot} can be expressed as $\Delta S_{\text{tot}} = \Delta S_{\text{M}} + \Delta S_{\text{st}}$ [17]. The Clausius-Clapeyron thermodynamic relation implies that $(dT_{\text{M}}/dP) = -(\Delta V/\Delta M)(dT_{\text{M}}/dB)$. The change in unit cell volume (ΔV) during the MST was estimated using the experimental values of $dT_{\text{M}}/dP = 1.43 \text{ K/kbar} = 1.43 \times 10^{-8} \text{ K/Pa}$, $dT_{\text{M}}/dB = -1.4 \text{ K/T}$, and $\Delta M = 55 \text{ emu/g} = 55 \text{ A m}^2/\text{kg}$ for $x=1$ (obtained from Fig. 3), yielding $\Delta V = 5.62 \times 10^{-7} \text{ m}^3/\text{kg}$. Taking into account the values of the lattice parameters as estimated from the room temperature XRD measurement ($a=5.76\text{\AA}$ and $c=6.41\text{\AA}$), $\Delta V/V$ has been calculated to be 0.11%. Employing the relationship between the change of ΔS_{st} and the relative volume change as $\delta(\Delta V/V(\%))/\delta(\Delta S_{\text{st}}) = 0.08 \text{ [J/kg K]}^{-1}$ [17], the value of ΔS_{st} was calculated using $\Delta V/V = 0.11\%$, which corresponds to a structural entropy contribution of $\Delta S_{\text{st}} = 1.42 \text{ J/kg K}$ for $x=1$. The value of ΔS_{st} turns out to be approximately 3.1% of the total entropy change ($\Delta S_{\text{tot}} = 46 \text{ J/kg K}$), indicating that the majority of the ΔS_{tot} originates from ΔS_{M} due to the change of the magnetic moment configuration. Therefore, the large switching-like change of MR under the application of low B ($\sim 16\%$ for $\Delta B=0.25 \text{ T}$ at 304 K for $x=1$) in this system indicates that the effect arises predominantly as a result of the spin-dependent scattering of conduction electrons.

V. CONCLUSIONS

As explored in this study, instead of the commonly reported athermal nature of both the reverse and forward metamagnetic transitions for this class of materials, the forward

metamagnetic transition from the FM austenitic to the PM-like martensitic was found to be isothermal with a pronounced magnetic relaxation, whereas the reverse one (from the PM-like martensitic to the FM austenitic phase) was observed as the usual athermal transition with a slow, glassy-type relaxation. As a result of the asymmetric metamagnetic transitions, an unusual and interesting type of switching-like change in the MR at low fields has been observed in the *bulk* system $\text{Ni}_{50}\text{Mn}_{35}\text{In}_{15-x}\text{B}_x$ with $x=1$ in the vicinity of the phase coexistence region. The change of MR reaches about 16% for a field change of $B=0\rightarrow 0.25$ T near room temperature (304 K). These results illuminate a new potential functionality of this class of Heusler alloys, and elucidate new information regarding the phase transitions (and phase stability) that are responsible for the multifunctional behaviors observed in Heusler alloys and related intermetallic systems.

ACKNOWLEDGMENTS

This work was supported by the Office of Basic Energy Sciences, Material Science Division of the U.S. Department of Energy (Grant Nos. DE-FG02-13ER46946 and DE-FG02-06ER46291).

References:

- [1] S. A. Wolf, D. D. Awschalom, R. A. Buhrman, J. M. Daughton, S. von Molnár, M. L. Roukes, A.Y. Chtchelkanova, and D. M. Treger, *Science* **294**, 1488 (2001).
- [2] C. Chappert, A. Fert, and F. N. V. Dau, *Nature Mater.* **6**, 813 (2007).
- [3] B. Dieny, *J. Magn. Magn. Mater.* **136**, 335 (1994).
- [4] J. S. Moodera, Lisa R. Kinder, Terrilyn M. Wong, and R. Meservey, *Phys. Rev. Lett.* **74**, 3273 (1995).
- [5] S. Tsunegi, Y. Sakuraba, M. Oogane, K. Takanashi, and Y. Ando, *Appl. Phys. Lett.* **93**, 112506 (2008).
- [6] W. P. Pratt, Jr., S. F. Lee, J. M. Slaughter, R. Loloee, P. A. Schroeder, and J. Bass, *Phys. Rev. Lett.* **66**, 3060 (1991).
- [7] Z. H. Xiong, D. Wu, Z. V. Vardeny, and J. Shi, *Nature* **427**, 821 (2004).
- [8] S. Singh, R. Rawat, S. E. Muthu, et al. *Phys. Rev. Lett.* **109**, 246601 (2012).
- [9] M. K. Chattopadhyay, S. B. Roy, and P. Chaddah, *Phys. Rev. B* **72**, 180401(R) (2005).
- [10] A. Eiling and J. S. Schilling, *J. Phys. F* **11**, 623 (1981).
- [11] B. R. Gautam, I. Dubenko, A. K. Pathak, S. Stadler, and N. Ali, *J. Phys.: Condens. Matter* **20**, 465209 (2008).
- [12] H. Luo, F. Meng, Q. Jiang, H. Liu, E. Liu, G. Wu, and Y. Wang, *Scr. Mater.* **63**, 569 (2010).
- [13] V. K. Sharma, M. K. Chattopadhyay, and S. B. Roy, *Phys. Rev. B* **76**, 140401(R) (2007).
- [14] S. Chatterjee, S. Giri, and S. Majumdar, *Phys. Rev. B* **77**, 012404 (2008).
- [15] S. Kustov, I. Golovin, M. L. Corró, and E. Cesari, *J. Appl. Phys.* **107**, 053525 (2010).
- [16] N. Sakamoto, T. Kyomen, S. Tsubouchi, and M. Itoh, *Phys. Rev. B* **69**, 092401 (2004).
- [17] K. A. Gschneidner, Jr. Y. Mudryka, and V. K. Pecharsky, *Scr. Mater.* **67**, 572 (2012).

Figure Captions:

Fig. 1 Room temperature XRD patterns for $\text{Ni}_{50}\text{Mn}_{35}\text{In}_{15-x}\text{B}_x$ with $x=1.0, 1.5,$ and 2.0 . Indexes “A” and “M” identify the XRD peaks from the austenitic and martensitic phases, respectively.

Fig. 2 Zero-field-cooled (ZFC) resistivity (ρ) as a function of temperature measured for $B=0$ and 5 T (left axis), and the temperature dependence of the magnetization (M) with $B=0.05$ T (right axis) near the MST for (a) $x=1.0,$ (b) $x=1.5,$ and (c) $x=2.0$.

Fig. 3 Magnetization as a function of temperature with $B=0.05$ T for an applied hydrostatic pressure (P) of 7.7 kbar and at ambient pressure for $x=1$ (left axis). $M(T)$ for $B=5$ T is referred to the right axis.

Fig. 4 (a) Temperature dependence of the magnetoresistance (MR) for a field change of $\Delta B=5$ T. Isothermal MR as a function of magnetic field measured at different constant temperatures in close vicinity to the respective MST for (b) $x=1.5$ and (c) $x=2$.

Fig. 5 The magnetic-field-dependent hysteresis of the magnetoresistance (MR) and magnetization (M) in the vicinity of the MST for $x=1$ measured at (a) $\text{MR}(B), T=300$ K, (b) $\text{MR}(B), T=302$ K, (c) $\text{MR}(B), T=304$ K, (d) $\text{MR}(B), T=305$ K, (e) $M(B), T=304$ K, and (f) $M(B), T=305$ K. The numbered arrows (1-6) labeling the various curves refer to the order of the measurements.

Fig. 6 Normalized magnetization ($M(t)/M(t=0)$) measured as a function of time (t) at $T=304$ K for different constant applied magnetic fields in the phase coexistence region for $x=1$. The field sequence before starting the relaxation measurement is highlighted in the legend. The logarithmic fitting of the relaxation data points are indicated by solid curves. (Inset:) The magnetic viscosity coefficient (Z) for the two types of metamagnetic transitions as estimated from the fitting of relaxation curves measured in the presence of different constant magnetic fields (B).

Fig. 7 Landau-type free-energy diagrams for the first-order phase transition, showing the evolution of the free-energy profiles in the case of (a) reverse and (b) forward metamagnetic transitions. ‘A’ and ‘M’ denote austenitic and martensitic minima, respectively. The dashed lines indicate the modification of austenitic and martensitic minima associated with the two different types of metamagnetic transitions, namely, “athermal” and “isothermal” transitions, respectively.

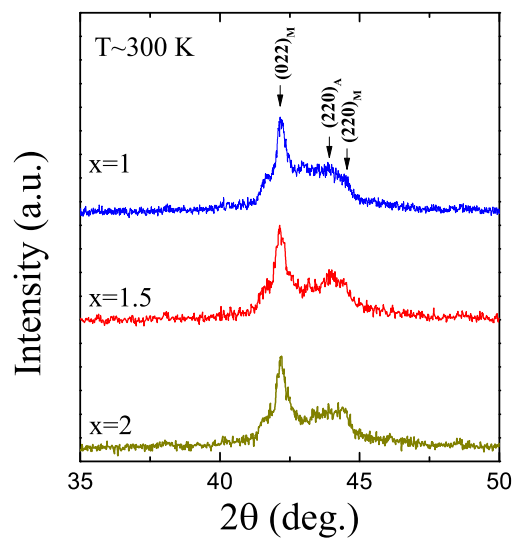


Figure 1

LS14647B

25JUL2014

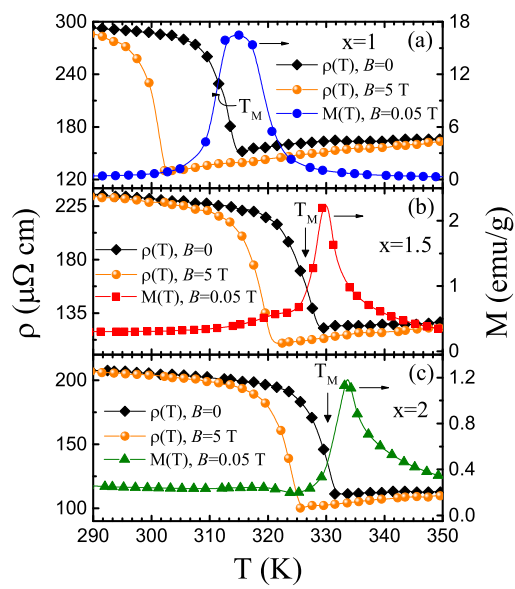


Figure 2

LS14647B

25JUL2014

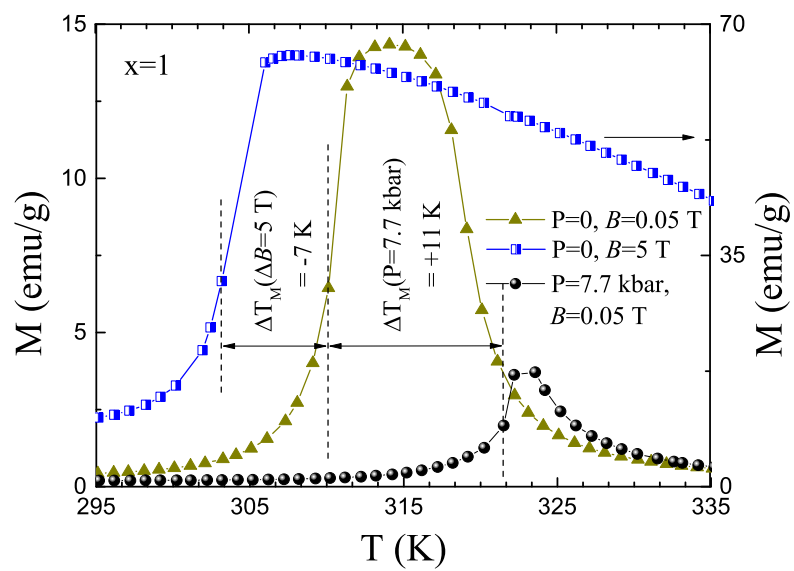


Figure 3 LS14647B 25JUL2014

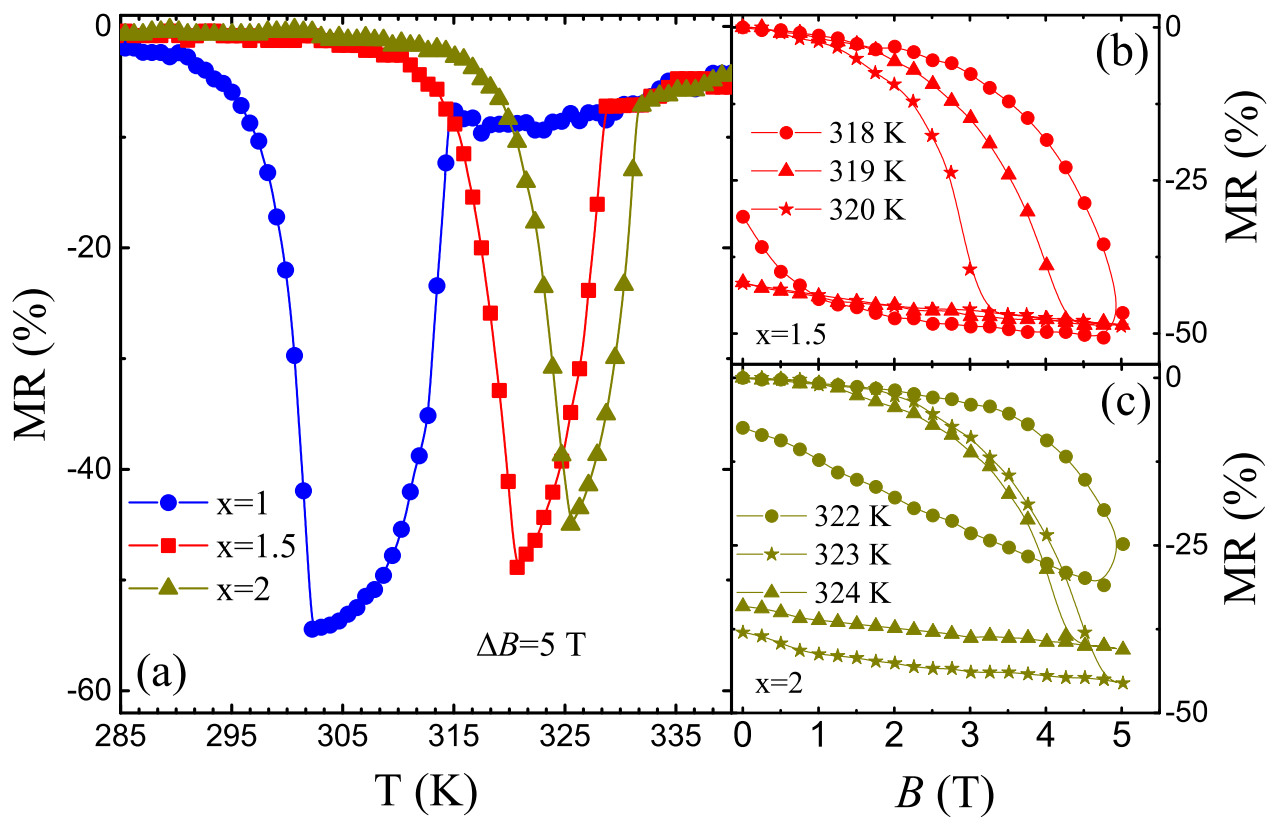


Figure 4

LS14647B

25JUL2014

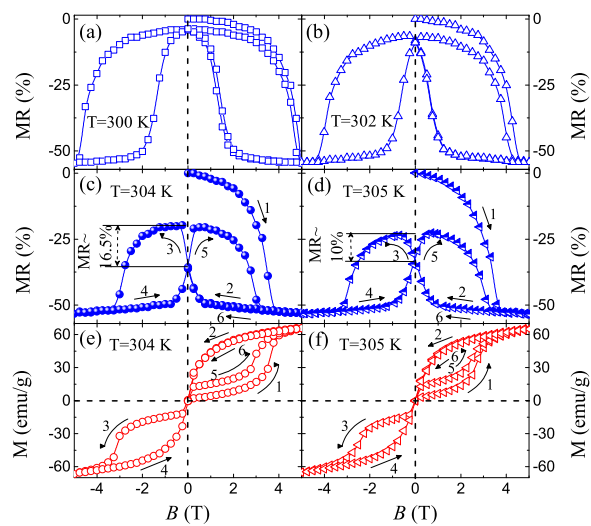
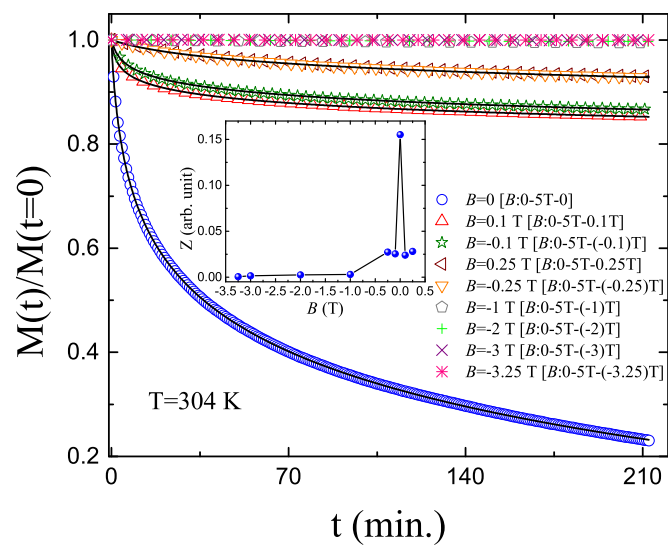


Figure 5

LS14647B

25JUL2014



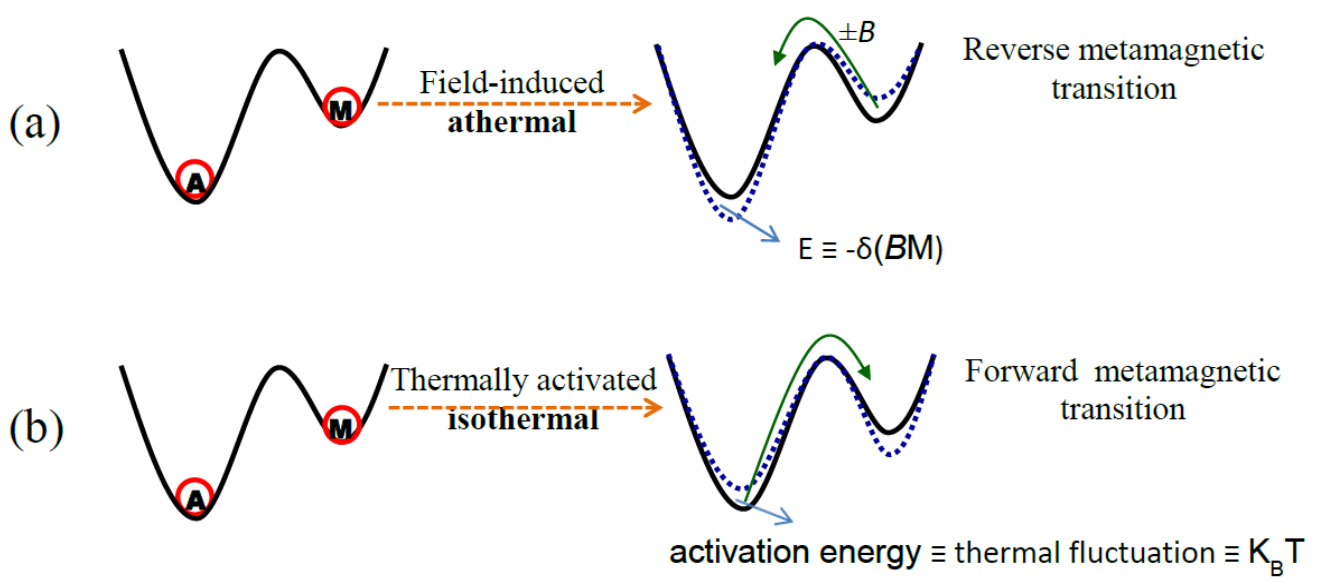


Figure 7 LS14647B 25JUL2014